10. R. A. Levy, M. L. Green, and P. K. Gallagher, *This Journal*, **131**, 2175 (1984).
11. H. W. Piekaar, L. F. Tz. Kwakman, and E. H. A. Granneman, in *Proceedings of the 6th International IEEE VLSI Multilevel Interconnection Conference,-1989*, p. 122, IEEE, New York (1989).
12. K. P. Cheung, C. J. Case, R. J. Schutz, R. S. Wagner, L. F. Tz. Kwakman, D. Huibregtse, H. W. Piekaar, and E. H. A. Granneman, in *Proceedings of the 7th International IEEE VLSI Multilevel Interconnection Conference,-1990*, p. 303, IEEE, New York (1990).
13. W. Y-C. Lai, K. P. Cheung, C. J. Case, D. P. Favreau, C. Case, R. Liu, R. G. Murray, L. F. Tz. Kwakman, and D. Huibregtse, in *Proceedings of the 8th International IEEE VLSI Multilevel Interconnection Conference-1991*, p. 89, IEEE, New York (1991).
14. K. Sugai, H. Okabayashi, A. Kobayashi, T. Yako, and S. Kishida, *Jpn. J. Appl. Phys.*, **34**, L429 (1995).
15. A. Kobayashi, K. Sugai, T. Yako, A. Sekiguchi, T. Shinzawa, S. Kishida, H. Okabayashi, H. Kadokura, O. Okada, and N. Hosokawa, in Extended Abstracts 55th Autumn Meeting of the Japan Society of Applied Physics, p. 722, The Japan Society of Applied Physics, Nagoya) (1994) [in Japanese].
16. K. Tsubouchi, K. Masu, N. Sigeeda, T. Matano, Y. Hiura, N. Mikoshiba, S. Matsumoto, T. Asaba, T. Marui, and T. Kajikawa, in Digest of Technical Papers, 1990 Symposium on VLSI Technology, p. 5 (1990).
17. G. A. Dixit, A. Paranjpe, Q. Z. Hong, L. M. Ting, J. D. Luttmer, R. H. Haveman, D. Paul, A. Morrison, K. Littau, M. Eizenberg, and A. K. Sinha, in Abstracts of International Electron Devices Meeting-1995, p. 1001, IEEE, Piscataway, NJ (1995).
18. K. Sugai, H. Okayashi, T. Shinzawa, S. Kishida, T. Kobayashi, N. Hosokawa, T. Yako, H. Kadokura, M. Isemura, and M. Naruse, Abstract 315, p. 482, The Electrochemical Society Meeting Abstracts, Vol. 93-1, Honolulu, HI, May 16-21, 1993.
19. K. Sugai, H. Okabayashi, T. Shinzawa, S. Kishida, T. Kobayashi, N. Hosokawa, T. Yako, H. Kadokura, M. Isemura, and M. Naruse, in *Proceedings of Symposia on Interconnects, Metallization, and Multilevel Metallization and Reliability for Semiconductor Devices, Interconnects and Thin Insulator Materials*, T. O. Herndon, H. O. Okabayashi, N. Alvi, H. S. Rathore, R. A. Susko, and M. Kashiwagi, Editors, PV 93-25, pp. 290-298, The Electrochemical Society Proceedings Series, Pennington, NJ (1993).
20. K. Sugai, H. Okabayashi, T. Shinzawa, S. Kishida, T. Kobayashi, N. Hosokawa, T. Yako, H. Kadokura, M. Isemura, and K. Kamio, in *Proceedings of the 10th International IEEE VLSI Multilevel Interconnection Conference-1993*, p. 463, IEEE, New York (1993).
21. A. Takamatsu, M. Shuto, and T. Yoshimi, Abstract 334, p. 501, The Electrochemical Society Meeting Abstracts, Vol. 86-2, San Diego, CA, Oct. 9-14, 1996.
22. K. Sugai, H. Okabayashi, T. Shinzawa, S. Kishida, A. Kobayashi, T. Yako, and H. Kadokura, *J. Vac. Sci. Technol.*, **B13**, 2115 (1995).
23. K. Sugai, T. Shinzawa, S. Kishida, and H. Okabayashi, in *Proceedings of 1991-4th MicroProcess Conference*, p. 206, Business Center for Academic Societies Japan, Tokyo (1991).
24. K. Sugai, H. Okabayashi, S. Kishida, and T. Shinzawa, *Thin Solid Films*, **280**, 142 (1996).
25. M. M. IslamRaja, M. A. Cappelli, J. P. McVittie, and K. C. Saraswat, *J. Appl. Phys.*, **70**, 7137 (1991).
26. A. Kobayashi, K. Sugai, A. Sekiguchi, S. Kishida, H. Okabayashi, T. Yako, T. Shinzawa, O. Okada, N. Hosokawa, and H. Kadodura, *Electron. Commun. Jpn.*, Part 2, **78**, No. 12, 50 (1995).

Electrochemical Properties of $BaCe_{0.8}Gd_{0.2}O_3$ Electrolyte Films Deposited on Ni-$BaCe_{0.8}Gd_{0.2}O_3$ Substrates

Vishal Agarwal* and Meilin Liu**

School of Materials Science and Engineering, Georgia Institute of Technology, Atlanta, Georgia 30332-0245, USA

ABSTRACT

Solid oxide fuel cells (SOFCs) based on $BaCe_{0.8}Gd_{0.2}O_3$ (BCG) electrolyte films are constructed and tested at intermediate temperatures (700 to 800°C) using hydrogen as fuel and air as oxidant. The ionic and electronic conductivities as well as the interfacial properties of the BCG electrolyte films, as deposited on Ni-BCG substrates, are also determined from impedance and open-cell voltage measurements. Results indicate that the performance of the fuel cells is very sensitive to materials selection and to processing. Diffusion of Ni from substrates into the BCG electrolyte films during processing increases not only the bulk and interfacial resistances but also the electronic transference numbers of the electrolyte films, resulting in reduced open-cell voltages and poor power output. The performance of solid oxide fuel cells based on BCG electrolyte films may be substantially improved, however, by avoiding Ni diffusion into BCG electrolyte through proper selection of materials and modifications in processing.

Introduction

Barium cerate-based materials exhibit relatively high ionic conductivities at intermediate temperatures (600 to 800°C) and are thus an attractive choice as electrolytes for intermediate-temperature solid oxide fuel cells.[1-3] Gd-doped barium cerate with a composition of $BaCe_{0.8}Gd_{0.2}O_3$ exhibits the highest conductivity among the barium cerate-based electrolytes studied.[2] Further, the long-term stability of the BCG electrolyte has been demonstrated under hydrogen-air fuel cell conditions[4,5] and in H_2O-containing conditions.[6] The performance of SOFCs, however, can be further enhanced by reducing the thickness of the BCG electrolyte.[4]

For successful construction of an SOFC based on a BCG electrolyte film, several technical challenges must be overcome. The electrolyte film must be dense and crack-free to avoid short-circuiting and fuel leakage; the electrodes must be electrically conductive, catalytically active, and porous (to facilitate gas transport); and the seals must be electrically insulating and gastight (to prevent leakage). In our earlier studies, a colloidal[7] and a modified Pechini[8] process were investigated to prepare BCG electrolyte films on various porous substrates. Electrically conductive and porous Ni-BCG disks were used as substrates for BCG films to facilitate the electrical characterization of these films. In addition, the use of Ni-BCG reduces the thermal expansion mismatch between the electrolyte film and the substrate.

In this study, single cells based on BCG electrolyte films, prepared on porous Ni-BCG substrates, were constructed and tested. Open-cell voltage (OCV), impedance spectra (IS), and current-voltage characteristics of each cell were acquired under various testing conditions to characterize the electrochemical properties of each cell component as well as the overall performance of each cell.

* Electrochemical Society Student Member.
** Electrochemical Society Active Member.

Experimental

Porous Ni-BCG composites were used as anode and as supporting substrates for preparation of BCG electrolyte films. The BCG powders used in the Ni-BCG composite were prepared by conventional ceramic processing.[9] To ensure that the substrate is electrically conductive, the composition of the composite was so chosen that the volume fraction of Ni metal would be 40% after reduction of NiO to Ni metal. Disks of NiO-BCG (1.7 cm diam and 1.5 mm thick) were prefired at 1000°C and BCG electrolyte films were subsequently deposited as described elsewhere.[7] Unfritted silver paste (Heraeus: C4400UF) was screen-printed on the top of each electrolyte film and fired at 800°C for 10 min to form a porous silver electrode. The samples were then attached to an alumina tube using a glass seal. A hermetic seal is crucial to the reliable testing of SOFCs. The sealing glass composition was chosen such that its thermal expansion coefficient lies between alumina and BCG and its softening point was above 800°C to form a hard seal at or below 800°C. The sealing glass consists of three glasses, glass A, glass V-960, and glass V805-B, with a weight ratio of 1:2:4. Glass A was prepared in our lab with the following composition: 49.3 weight percent (w/o) SiO_2, 17.7 w/o Na_2O, 13.7 w/o B_2O_3, 7.6 w/o CaO, 6.8 w/o Al_2O_3, 3.7 w/o K_2O, 0.66 w/o Li_2O, 0.3 w/o MnO_2, and 0.24 w/o Co_2O_3.[10] Glasses V-960 and V805-B were obtained from Vitrifunction. The glasses were fired *in situ* and the heating and cooling rates were carefully controlled to avoid cracking of the glass seal. The furnace was heated at 7°C/min to 840°C, held at the temperature for 5 min to soften the glass, and then cooled down at 1.5°C/min to the desired temperature for testing.

A scheme of the cell test apparatus is shown in Fig. 1. After the glass seals were fired *in situ*, argon was supplied to the anode while the cathode was exposed to ambient air. Approximately 30 min after the cell reached the operating temperature (700 to 800°C), the anode gas was switched to hydrogen (water content about 1 volume percent (v/o)) to reduce NiO in the porous substrate to Ni metal. At 800°C, NiO was completely reduced to Ni in about 1 h.

Impedance spectra of the cells were obtained at temperatures ranging from 700 to 800°C in the frequency range from mHz to MHz using a computerized impedance analysis system consisting of a frequency response analyzer (Solatron 1255) and an electrochemical interface (Solatron 1286). The OCVs and current-voltage characteristics were also recorded under identical conditions for each impedance measurement.

A Hitachi S-800 scanning electron microscope (SEM) was used to characterize the microstructures of cells before and after cell operation. A statistical "point counting" method in quantitative stereology[11] was used to estimate the porosities of substrates and electrodes.

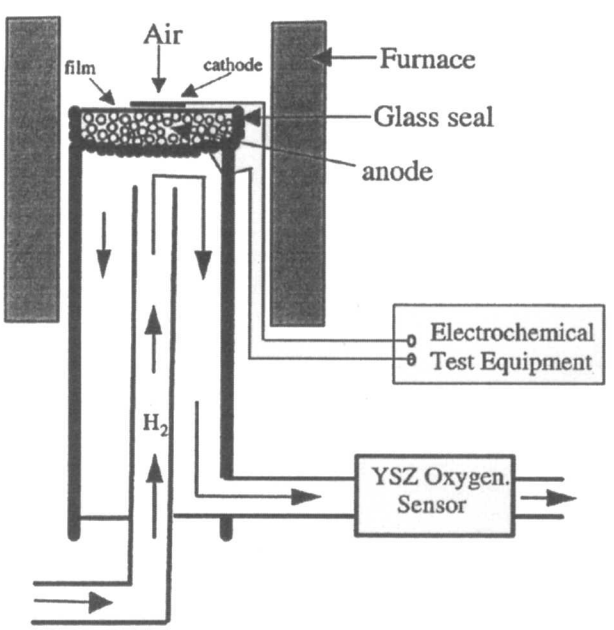

Fig. 1. A schematic showing the experimental arrangement for fuel cell testing.

Results and Discussion

Microstructure.—Figure 2a shows a cross-sectional view of a BCG film (sintered at 1200°C for 2 h) on a NiO-BCG

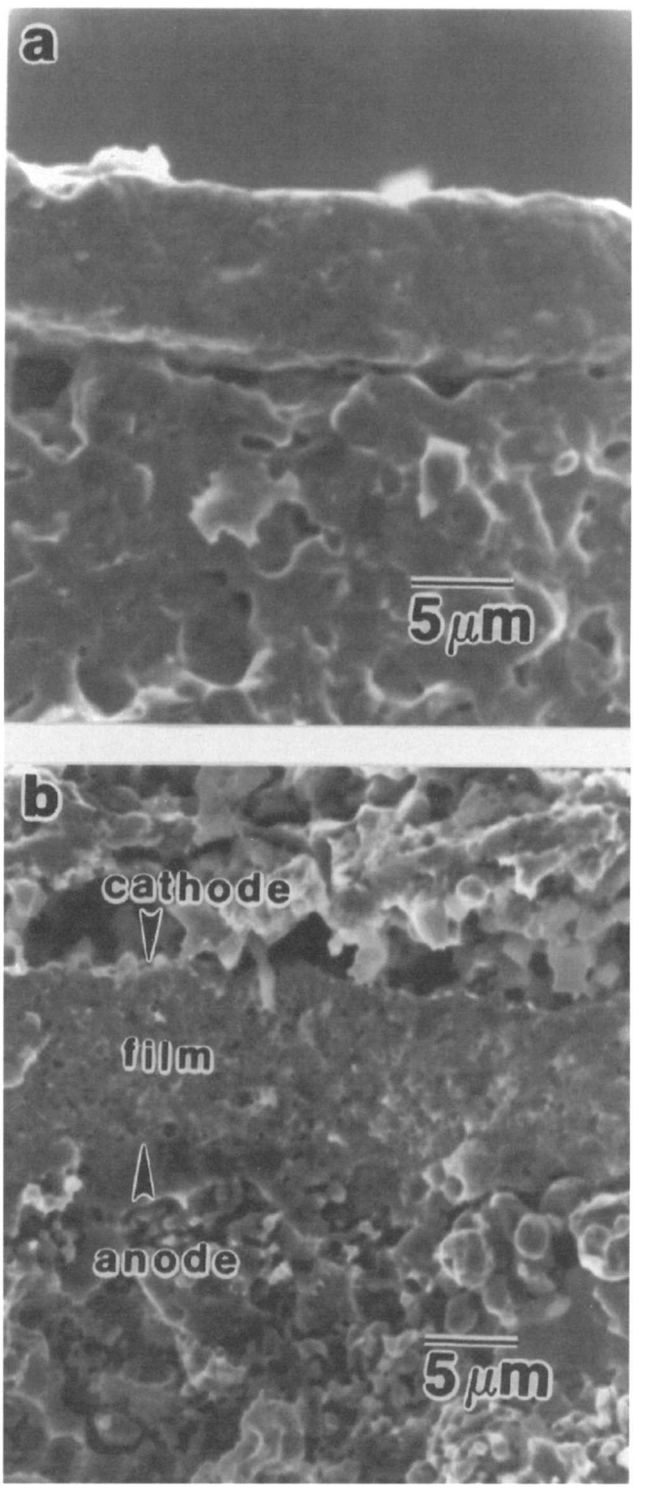

Fig. 2. Cross-sectional views of (a) a BCG film on the top of a NiO-BCG substrate and (b) a single cell after 150 h of operation at 750°C. The lower layer was a porous Ni-BCG anode, the middle layer was a nonporous BCG electrolyte film, and the top layer was a porous Ag cathode.

substrate. The micrograph indicates that the film was dense and the grain size ranged from 1 to 3 μm. The thickness of the film was about 8 to 9 μm, which was derived from two consecutive coatings. The porosity of the NiO-BCG substrate was estimated to be about 10% before reduction. Figure 2b shows a cross-sectional view of a fuel cell after 150 h of operation at 750°C. The top layer was a porous Ag cathode, the middle layer was a nonporous electrolyte film, and the bottom layer was a porous Ni-BCG substrate. There were no observable changes in microstructure of the electrolyte film after testing, implying that the microstructure of the electrolyte film is stable. The estimated porosity of the Ni-BCG anode, however, increased to 25% due to the additional porosity created by the reduction of NiO to Ni metal. The porosity of the Ag cathode was estimated to be about 22%. The highly porous structure of the anode and the cathode is desirable for gas transport during cell operation.

Electrochemical properties of BCG films.—*Open-cell voltage.*—Figure 3 shows the OCVs of fuel cells based on different electrolytes as constructed in Fig. 1. Clearly, the OCVs of the cells based on BCG films were lower than that of the cells based on BCG pellets.[12] Three factors may influence the observed OCV across a BCG film on a Ni-BCG substrate: (*i*) the presence of Ni in the film,[7] (*ii*) reduced thickness of the BCG film, and (*iii*) gas leakage through the glass seals. The readings of the yttria-stabilized zirconia (YSZ) oxygen sensor indicated that there was very little gas leakage through the glass seals; thus, the presence of Ni in the BCG films may reduce the OCV values by decreasing the ionic transference number of the electrolyte. In order to determine if Ni doping has any effect on observed OCVs, the transport properties of the BCG films were characterized.

Bulk resistance.—Typical impedance spectra of single cells based on BCG films are shown in Fig. 4. The intercepts of the impedance locus with the real axis at high frequencies correspond to the bulk resistances (R_b) of the electrolyte film, while the intercepts at low frequencies correspond to the total resistances (R_T) of the cell. Plotted in Fig. 5 are the bulk conductivities of BCG films, which were calculated from the bulk resistances as determined from the impedance spectra. For comparison, the data for a BCG pellet with and without Ni[13] are also plotted in Fig. 5. It can be seen that the conductivities of the BCG films on Ni-BCG substrates are very close to (slightly higher than) those of the Ni-doped BCG pellets but nearly one order of magnitude lower than those of BCG pellets (without Ni).[13] Thus, it is reasonable to state that Ni significantly reduces the conductivity of BCG electrolyte, even though the exact amount of Ni in the film is unknown.

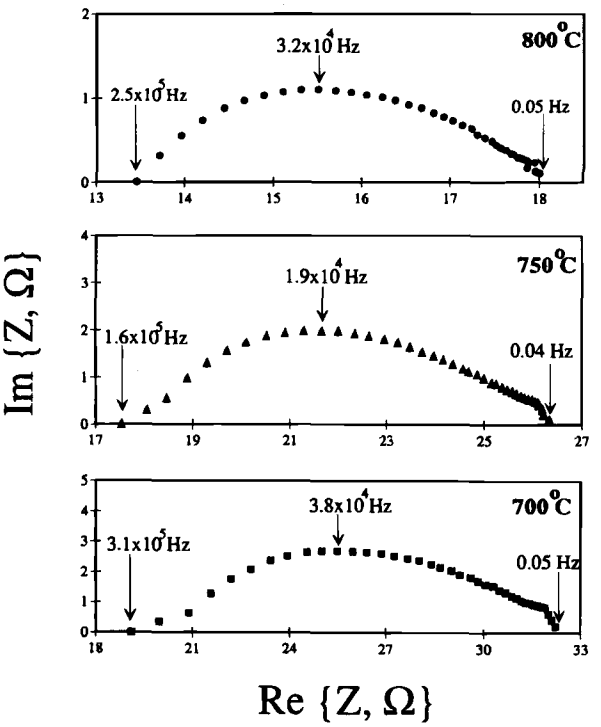

Fig. 4. Impedance spectra of fuel cells based on BCG electrolyte films measured at different temperatures (electrode area 0.1 cm², electrolyte thickness 12 μm).

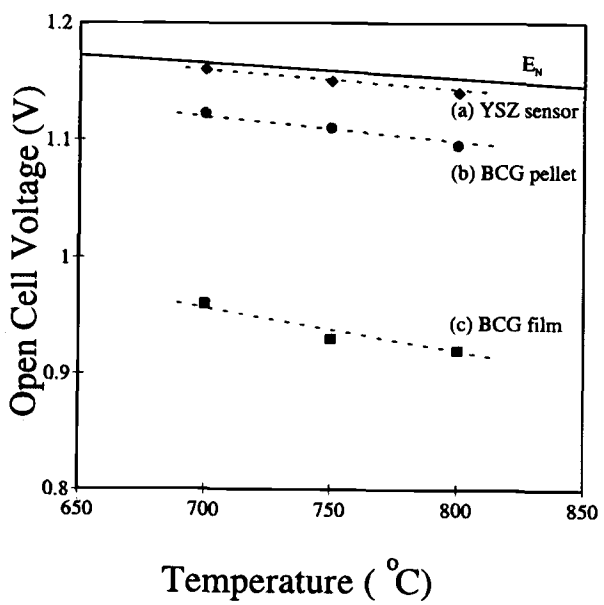

Fig. 3. Nernstian potential (E_N) and open-cell voltages of fuel cells based on different electrolytes: (a) YSZ, (b) BCG electrolyte pellet without Ni, and (c) BCG film deposited on Ni-BCG substrates. The cells were exposed to air on one side and to hydrogen (1 v/o H_2O) on the other side.

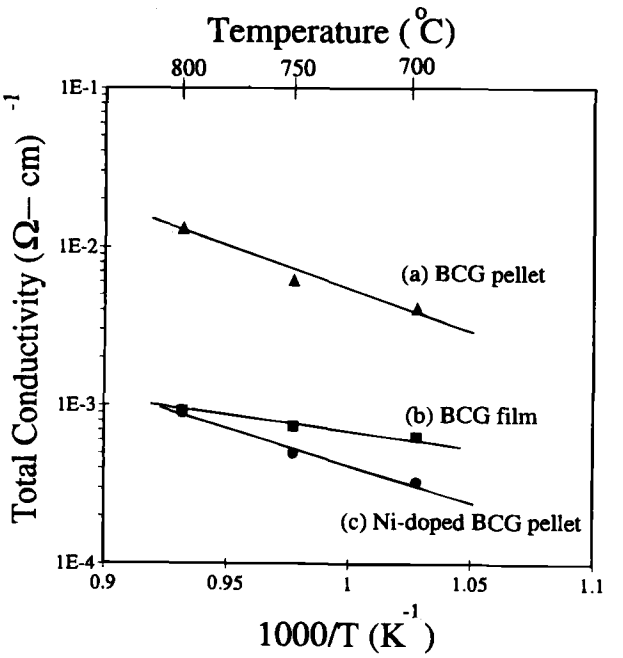

Fig. 5. Temperature dependance of the total conductivities of different electrolytes tested under H_2-air fuel cell conditions: (a) BCG pellet, (b) BCG film (with a small amount of Ni), and (c) Ni-doped BCG pellet ($BaCe_{0.8}Gd_{0.1}Ni_{0.1}O_3$).

Interfacial resistance.—When the electrolyte of a cell has considerable electronic conduction, the polarization resistance (Ω) of the interfaces (R_p) can be calculated from the following equation[14]

$$R_p = \frac{R_T - R_b}{\frac{V_{oc}}{E_N}\left[1 - \frac{R_b}{R_T}\left(1 - \frac{V_{oc}}{E_N}\right)\right]} \quad [1]$$

where R_T is the total resistance of the cell, R_b is the resistance of the bulk electrolyte, V_{oc} is the open-cell voltage, and E_N is the Nernstian potential applied to the cell.

Shown in Fig. 6 are the specific interfacial resistances (Ω cm^2) of a fuel cell based on a BCG film on a Ni-BCG substrate with a configuration of air, Ag/BCG/Ni-BCG,H_2(1 v/o H_2O). For rough comparison, the specific interfacial resistances of two symmetrical cells based on BCG pellets (without Ni) are also plotted in the same figure, one cell using pure Ag electrodes and the other using Ag-BCG composite electrodes (with composition of 62 v/o Ag and 38 v/o BCG).[15] The symmetrical cells were tested in air in a four-electrode configuration.[15] The specific interfacial resistances of the cell based on a BCG film on a Ni-BCG substrate, Ni-BCG/BCG/Ag, are about twice those of the symmetrical cell of Ag/BCG(pellet)/Ag, and about twenty times those of the symmetrical cell of Ag-BCG/BCG(pellet)/Ag-BCG. These data indicate that interfacial resistances are very sensitive to materials selection and to processing. Interfacial resistances can be orders of magnitude higher if the electrodes are improperly chosen or processed. It is crucial to have an electrode that is not only physically and chemically compatible with the electrolyte, but also electrically conductive, catalytically active, and can be made porous. The use of Ag-BCG composite cathodes for the BCG films may result in lower interfacial resistance and, hence, improved performance.

Shown in Fig. 7 are the bulk (R_b) and interfacial (R_p) resistance of a cell based on a BCG film deposited on a Ni-BCG substrate. The interfacial resistance increased rapidly as temperature was reduced because of large activation energies for interfacial processes.[15] The "crossover temperature" is about 685°C, below which the interfacial resistance is greater than the bulk resistance. Accordingly, if the operating temperature is above the crossover temperature, efforts should focus on reducing the bulk resistance to improve the overall performance of the cell effectively. Below the crossover temperature, however, attempts to reduce the interfacial resistance would be more effective in improving the overall performance of the cell. In general, the interfacial resistance plays a dominant role in determining the performance of a device based on a thin-film electrolyte and operated at low temperatures. One way to reduce the interfacial resistance is to engineer the microstructure of the interfaces. The use of Ag-BCG composite electrodes, for instance, is proven to be chemically and physically compatible with BCG electrolyte and shows improved performance over silver electrodes.[15]

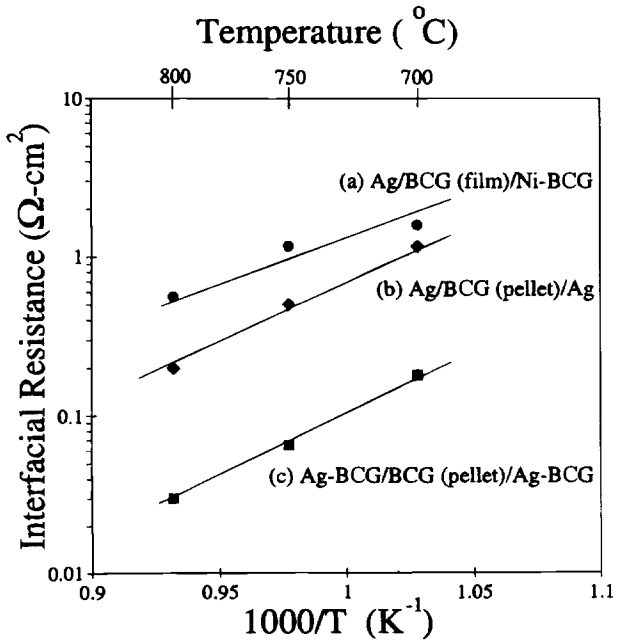

Fig. 6. Temperature dependance of the specific interfacial resistances of (a) a fuel cell based on a BCG film on a Ni-BCG substrate (*i.e.*, H_2,Ni-BCG | BCG(film) | Ag,air) and two symmetrical cells based on BCG pellets with different electrodes: (b) air, Ag | BCG | Ag, air, and (c) air, Ag-BCG | BCG | Ag-BCG, air.

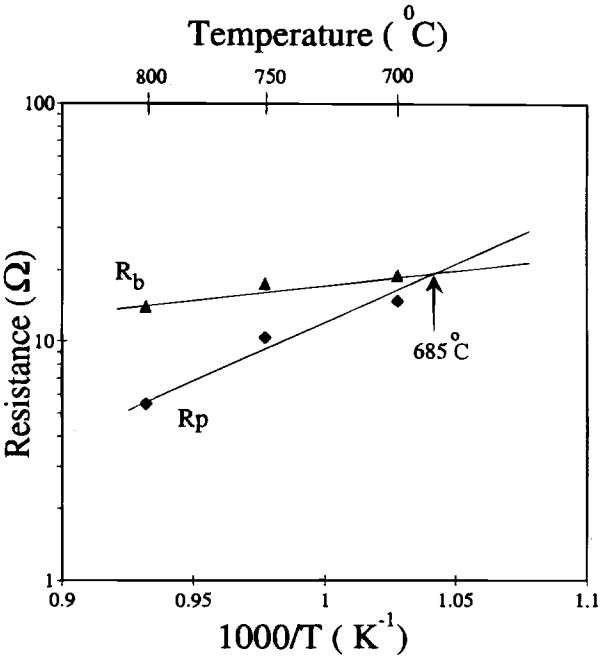

Fig. 7. Temperature dependance of the bulk and interfacial resistances of a fuel cell based on a BCG electrolyte film. The cell was tested under H_2-air fuel cell conditions (electrode area was 0.1 cm^2 and electrolyte thickness was 12 μm).

Transference number.—From this discussion it is clear that the presence of Ni in the electrolyte increased both bulk and interfacial resistances of the electrolyte. Further, it is more instructive to know the effect of Ni on the ionic (R_i) and electronic (R_e) resistance of the BCG electrolyte film using the following equations[14]

$$R_i = \frac{R_b R_e}{R_e - R_b} \quad [2]$$

$$R_e = \frac{R_T}{1 - \frac{V_{oc}}{E_N}} \quad [3]$$

where the OCV measurements and the impedance measurements must be performed under identical conditions.[14]

The estimated ionic and electronic conductivities are plotted in Fig. 8a. It can be seen that the electrolyte films exhibit considerable electronic conduction (10 to 15%). The ionic transference number (t_i) as defined by

$$t_i = \frac{R_e}{R_i + R_e} \quad [4]$$

can be further calculated from R_i and R_e. Figure 8b shows the ionic transference numbers and V_{oc}/E_N ratios for BCG pellets (without Ni)[12] and for BCG films deposited on Ni-BCG substrates as measured at different temperatures. It

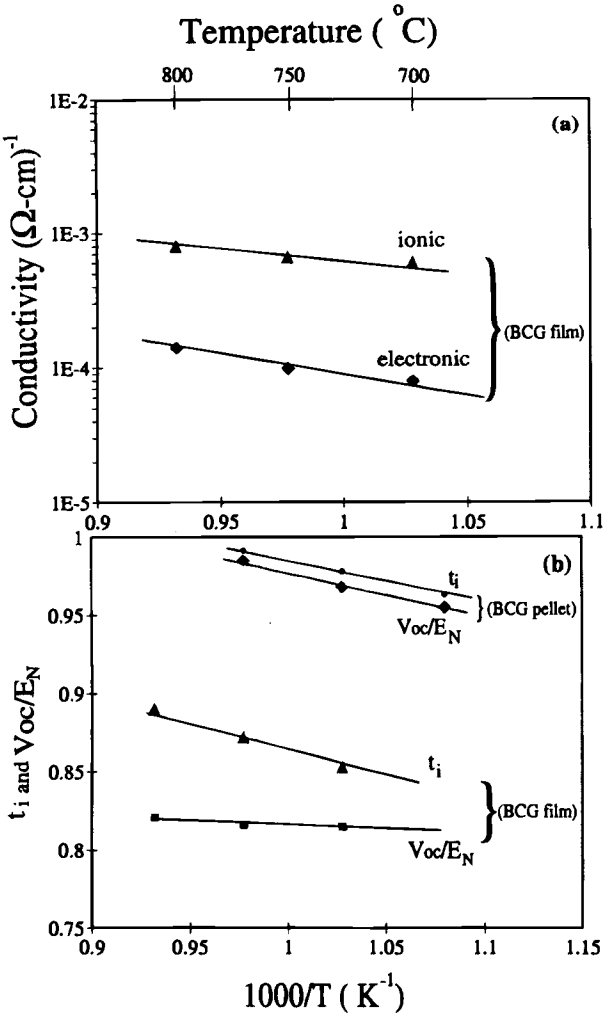

Fig. 8. Temperature dependance of (a) the ionic and electronic conductivities and (b) the calculated ionic transference numbers and V_{oc}/E_N ratios of BCG electrolyte films tested under H_2-air fuel cell conditions.

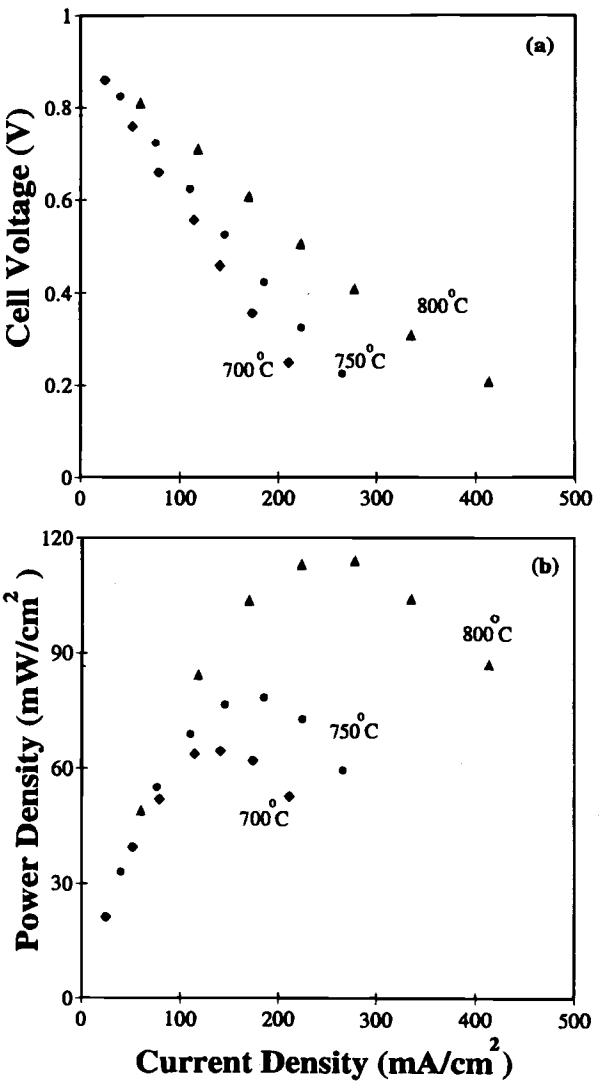

Fig. 9. Typical (a) current-voltage characteristics and (b) power densities of a fuel cell based on a BCG electrolyte film tested in H_2-air fuel cell conditions.

can be seen that the ionic transference numbers of the BCG films (with a small amount of Ni) are lower than those of the BCG pellets. This strongly suggests that the presence of Ni decreases ionic conductivity and increases the electronic transference number of the electrolyte, which reduces OCVs and is detrimental to the performance of fuel cells based on the electrolyte. Another interesting observation is that the deviations of ionic transference numbers from V_{oc}/E_N ratios are larger for BCG films than for the BCG pellet. This is due to the effect of interfacial resistance and electrolyte thickness, as explained elsewhere.[14]

Fuel cell performance.—Figure 9 shows the current-voltage characteristics of a cell in the temperature range from 700 to 800°C. As seen in the plot, a current density of about 280 mA/cm^2 was obtained at 800°C when the cell voltage was 0.4 V. At the same cell voltage, the current density was about 200 mA/cm^2 at 750°C and 160 mA/cm^2 at 700°C. The estimated total resistances of the cell (R_T) from the *I-V* plots in Fig. 9a agree well with the R_T value estimated from the impedance spectra in Fig. 4. The corresponding power densities of the cell are shown in Fig. 9b. The peak power output was approximately 113 mW/cm^2 at 800°C. The observed low current and power densities can be attributed to the observed degradation in bulk and interfacial properties of the electrolyte film due to the diffusion of Ni into the BCG electrolyte. Thus, significant improvements in cell performances may be possible if the diffusion of Ni into BCG electrolyte can be prevented during processing. For instance, the power density would be expected to increase by one order of magnitude just by preventing Ni from diffusing into the BCG electrolyte and by the use of an Ag-BCG composite electrode.

Conclusions

SOFCs based on $BaCe_{0.8}Gd_{0.2}O_3$ electrolyte films deposited on Ni-BCG substrates were constructed and tested under hydrogen-air fuel cell conditions. The diffusion of Ni from the substrate into the electrolyte film not only increased the bulk and interfacial resistances of the electrolyte but also reduced the ionic transference number of the electrolyte film, resulting in reduced OCV. The ionic transference numbers deviate from the V_{oc}/E_N ratios due to the effect of interfacial resistances. Low conductivities of the electrolyte film and high resistances of the interfaces resulted in poor cell performance. While the feasibility of construction and operation of SOFCs based on BCG electrolyte films on porous substrates has been demonstrated, many challenges still remain to improve the performance of the cells through modifications in processing or materials selection.

Acknowledgments

This work was supported by Electric Power Research Institute (EPRI) under Contract No. RP 1676-19 and by National Science Foundation (NSF) under Award No.

DMR-9357520, and their financial support of this research is gratefully acknowledged.

Manuscript submitted Sept. 6, 1996; revised manuscript received Nov. 22, 1996.

REFERENCES

1. N. Bonanos, B. Ellis, K. S. Knight, and M. N. Mahmood, *Solid State Ionics*, **35**, 179 (1989).
2. N. Taniguchi, K. Hatoh, J. Niikura, and T. Gamo, *ibid.*, **53-56**, 998 (1992).
3. H. Iwahara, *Solid State Ionics*, **52**, 111 (1992).
4. N. Taniguchi, E. Yasumoto, and T. Gamo, *This Journal*, **143**, 1886 (1996).
5. N. Bonanos, B. Ellis, and M. N. Mahmood, *Solid State Ionics*, **44**, 305 (1991).
6. Z. L. Wu and M. Liu, *This Journal*, Submitted.
7. V. Agarwal and M. Liu, *ibid.*, **143**, 3239 (1996).
8. V. Agarwal and M. Liu, *J. Mater. Sci.*, **32**, 619 (1997).
9. W. Rauch and M. Liu, in *Role of Ceramics in Advanced Electrochemical Systems*, P. N. Kumta, G. S. Rohrer, and U. Balachandran, Editors, *Ceramic Transactions*, Vol. 65, p. 73, The American Ceramic Society, Westerville, OH (1996).
10. W. Rauch, H. Hu, V. Agarwal, Z. Wu, and M. Liu, Unpublished work.
11. E. E. Underwood, in *Quantitative Microscopy*, p. 94, Addison Wesley Publ. Co., Reading, MA (1968).
12. H. Hu and M. Liu, Unpublished work.
13. W. Rauch and M. Liu, in *Ceramic Membranes I*, H. U. Anderson, A. C. Khandkar, and M. Liu, Editors, PV 95-24, p. 146, The Electrochemical Society Proceedings Series, Pennington, NJ (1997).
14. M. Liu and H. Hu, *This Journal*, **143**, L109 (1996).
15. H. Hu and M. Liu, *ibid.*, **143**, 859 (1996).

Ionic Transport Properties of Mixed Conductors: Application of AC and DC Methods to Silver Telluride

R. Andreaus[a] and W. Sitte*[,b]

[a]*Institut für Chemische Technologie Anorganischer Stoffe, and* [b]Institut für Physikalische und Theoretische Chemie, *Technische Universität Graz, A-8010 Graz, Austria*

ABSTRACT

The chemical diffusion coefficient and the ionic conductivity of the fast mixed conductor α'-$Ag_{2+\delta}Te$ have been measured with high stoichiometric resolution at 160 and 200°C within the range of homogeneity by applying both ac and dc methods. All measurements were performed on the same symmetric electrochemical cell. The stoichiometry of α'-$Ag_{2+\delta}Te$ was varied *in situ* by coulometric titration with AgI as a solid ionic conductor. Chemical diffusion coefficients and silver ionic conductivities are available from the transient voltage response of the ionic probes during polarization/depolarization experiments as well as from an analysis of the impedance data using an equivalent circuit model. The ac and dc results regarding the composition dependence of the chemical diffusion coefficient and the ionic conductivity of α'-$Ag_{2+\delta}Te$ are in full agreement with each other within the limits of error.

Introduction

Due to their high cationic and electronic conductivities as well as their high chemical diffusion coefficients, the medium temperature phases of the silver chalcogenides (α' phases) may be regarded as model substances for mixed conducting materials. The α' phase represents one of two structurally cationic disordered, mixed conducting phases of Ag_2Te.[1] The $\beta \rightarrow \alpha'$ phase transition occurs at about 132 to 145°C.[2]

Transport properties of mixed conductors in various solid-state electrochemical cells have been determined by dc and ac techniques, and reviews are available for dc (transient)[3,4] as well as ac techniques.[5-8] Maier[9] gives a review on various solid-state electrochemical dc and ac techniques, taking into account internal defect chemical reactions. Honders *et al.*[10-12] measured chemical diffusion coefficients and thermodynamic factors of solid solution electrode materials by ac and dc methods. Recently, the theory of galvanostatic processes in mixed conductors employed in asymmetric cells has been extended to the general case of arbitrary eletronic transport numbers of the mixed conductor.[13]

In this study we report on the agreement between the results of ac and dc measurements regarding the determination of the chemical diffusion coefficient and the ionic conductivity of the mixed conductor α'-$Ag_{2+\delta}Te$ using a recently developed solid-state electrochemical cell.[14] Both chemical diffusion coefficients and ionic conductivities are obtained at 160 and 200°C as a function of composition, the latter being varied by coulometric titration in the solid state. The advantage of our cell is that the ionic probes are located at the opposite ends of the mixed conducting sample; therefore, problems with the exact determination of their geometrical position (due to, *e.g.*, "soft" electrolyte edges) can be avoided. Some preliminary results obtained with this cell are given in Ref. 15.

* Electrochemical Society Active Member.

Theory

Electrochemical cell.—All ac and dc experiments were performed on the same symmetric solid-state cell equipped with two ionic electrodes and probes at the opposite ends of the sample

$$\mathrm{Ag}\left|\frac{\mathrm{AgI}}{\mathrm{Ag_{ref}}}\right|\alpha' - \frac{\mathrm{Ag_{2+\delta}Te}}{\mathrm{Pt}}\left|\frac{\mathrm{AgI}}{\mathrm{Ag_{ref}}}\right|\mathrm{Ag} \qquad [\mathrm{I}]$$

An additional platinum contact on the sample allows electromagnetic force (EMF) measurements and the *in situ* variation of the silver content of α'-$Ag_{2+\delta}Te$ by means of coulometric titration within the whole range of composition.

DC method.—The chemical diffusion coefficient, $\tilde{D}$, and the partial silver ionic conductivity σ_{ion} can be calculated from the dc voltage response $U(t)$ of the silver reference electrodes (Ag_{ref}). For the polarization process (after switching on a constant current at $t = 0$ and for times $t \geq \tau/2$) we obtain the following voltage response[14]

$$U_p(t) - U_p(t = \infty) = \frac{8}{\pi^2}\frac{jLt_e}{\sigma_{ion}}\exp\left(-\frac{t}{\tau}\right) \qquad [1]$$

with

$$U_p(t = \infty) = -\frac{jL}{\sigma_{ion}} \qquad [2]$$